INTERNATIONAL JOURNAL FOR NUMERICAL METHODS IN ENGINEERING, VOL, 36, 1395–1412 (1993)

A PENALTY FINITE ELEMENT METHOD FOR NON-NEWTONIAN CREEPING FLOWS

RAMON CODINA, MIGUEL CERVERA AND EUGENIO OÑATE

Escola Tècnica Superior d'Enginyers de Camins, Canals i Ports, Universitat Politècnica de Catalunya, Gran Capità s/n, Mòdul C1, 08034 Barcelona, Spain

SUMMARY

In this paper we present an iterative penalty finite element method for viscous non-Newtonian creeping flows. The basic idea is solving the equations for the difference between the exact solution and the solution obtained in the last iteration by the penalty method. For the case of Newtonian flows, one can show that for sufficiently small penalty parameters the iterates converge to the incompressible solution. The objective of the present work is to show that the iterative penalization can be coupled with the iterative scheme used to deal with the non-linearity arising from the constitutive law of non-Newtonian fluids. Some numerical experiments are conducted in order to assess the performance of the approach for fluids whose viscosity obeys the power law.

INTRODUCTION

The use of the penalty method for the finite element solution of incompressible flow problems has attracted the attention of many researchers. Its popularity is mainly due to the fact that it reduces the number of nodal unknowns of the problem. On the other hand, if the pure incompressible mixed velocity–pressure formulation is adopted, the element stiffness matrix of the discrete finite element problem has zero diagonal terms. Most of the standard finite element direct solvers use the elements of the diagonal as pivots.[1] In this case, renumbering algorithms have to be modified in order to prevent the appearance of zeroes in the diagonal of the assembled matrix when reducing the equations in the solution process. This results in the increase of the bandwidth of the global matrix. This problem is circumvented if the incompressibility constraint is penalized.

The main drawback of the penalty method is the ill-conditioning of the stiffness matrix when the penalty parameter is very small. For Newtonian flows, a fairly wide range of values of this parameter are known to yield good results (that is, the incompressibility equation is sufficiently well approximated) and to be easily handled if direct solvers are employed. Experience shows that the range $\varepsilon = 10^{-6}\mu^{-1}$ to $\varepsilon = 10^{-9}\mu^{-1}$ is recommended.[2,3] Here and below, ε denotes the penalty number and μ the dynamical viscosity of the fluid. Two questions arise. The first is what happens for non-Newtonian flows. In this case, the viscosity may vary several orders of magnitude in the fluid domain, especially if the physical properties of the material are considered to be thermally sensitive. The above rule for choosing the penalty parameter has to be applied using the smallest value of the viscosity (in order to avoid ill-conditioning), which is unknown before the calculation. Besides that, the incompressibility constraint will be excessively relaxed in the high-viscosity zones. Another question to be considered is whether iterative solvers can be safely used or not. Usually, their convergence is very sensitive to the condition number of the stiffness matrix, which grows as the penalty parameter decreases. When the effect of the non-constant viscosity is

0029–5981/93/081395–18$14.00

Received 15 November 1991
Revised 11 August 1992

present and iterative solvers are used, the behaviour of the standard penalty method is certainly disappointing.[4]

The objective of this paper is to present an iterative penalty finite element method whose basic motivation is alleviating the problems mentioned above. The incompressibility equation is penalized in each iteration but the residual of the previous iterate is added as a forcing term. For the case of the Stokes problem with constant viscosity, the convergence properties of the method are proved in Reference 5 and are also briefly stated here. The interesting issue is what happens when the iterative penalization is coupled with the iterative procedure due to the non-linearity of the problem. The case in which this non-linearity comes from the momentum equation (Navier–Stokes problem) is studied in detail in Reference 5 when the Picard and the Newton–Raphson algorithms are employed. Our purpose now is to present the method in the general framework of thermally coupled flows of non-linear fluids. We will focus our attention in non-Newtonian creeping flows. In the last part of the paper, some numerical experiments concerning the well-known 4:1 plane extrusion test for a fluid whose viscosity obeys the power law are presented.

BASIC EQUATIONS FOR THERMALLY COUPLED QUASI-NEWTONIAN FLOWS

Conservation equations and constitutive model

In what follows, we will consider only low Reynolds number steady-state flows. In this case, the time evolution and inertial terms in the Navier–Stokes equations can be neglected. The problem to be solved is to find a velocity field $\mathbf{u}$ and a pressure p such that

$$-2\nabla\cdot(\mu\boldsymbol{\varepsilon}(\mathbf{u}))+\nabla p=\rho\mathbf{f} \quad \text{in } \Omega \tag{1}$$

$$\nabla\cdot\mathbf{u}=0 \quad \text{in } \Omega \tag{2}$$

where $\nabla\cdot(\cdot)$ is the divergence operator, $\nabla(\cdot)$ the gradient operator, $\boldsymbol{\varepsilon}(\mathbf{u})$ the symmetric part of $\nabla\mathbf{u}$, ρ the material density, $\mathbf{f}$ the exterior body force and Ω a bounded domain in $\mathbb{R}^{N_{sd}}$ ($N_{sd}=2$ or 3). Whenever the viscosity μ is constant, equation (1) can be simplified using equation (2). The viscous term can be written as $-\mu\Delta\mathbf{u}$, where $\Delta(\cdot)$ is the Laplacian operator. However, the expression $-2\nabla\cdot(\mu\boldsymbol{\varepsilon}(\mathbf{u}))$ will be kept since we are interested in non-constant viscosities.

Equation (1) comes from the conservation of momentum, assuming the constitutive law of generalized Newtonian fluids

$$\boldsymbol{\sigma}=-p\mathbf{I}+2\mu\boldsymbol{\varepsilon}, \tag{3}$$

$\boldsymbol{\sigma}$ being the stress tensor and $\mathbf{I}$ the unit tensor. In general, μ will be a function of the invariants of $\boldsymbol{\varepsilon}$. Equation (2) states the conservation of mass for an incompressible material. In this case, the mechanical and thermal behaviour of the fluid is completely described by equation (1), (2) and the energy balance, that leads to the convection–diffusion equation for the temperature field θ:

$$\rho c\mathbf{u}\cdot\nabla\theta-k\Delta\theta=Q \tag{4}$$

Here, we have considered a constant and isotropic thermal conductivity k. The constant c in equation (4) is the specific heat and Q is the source term. Only the source coming from the mechanical dissipation into heat will be taken into account. Using equation (2), it is given by

$$Q=\boldsymbol{\sigma}:\boldsymbol{\varepsilon}=2\mu\varepsilon_{ij}(\mathbf{u})\varepsilon_{ij}(\mathbf{u}) \tag{5}$$

Boundary conditions have to be appended to problem (1)–(2)–(4). Let Γ be the boundary of Ω, split into two sets of disjoint components $\Gamma=\Gamma_{du}\cup\Gamma_{nu}$ and $\Gamma=\Gamma_{dt}\cup\Gamma_{nt}$. Let $\mathbf{n}$ be the unit vector

normal to Γ, $\mathbf{u}_0$ the velocity prescribed on Γ_{du}, $\mathbf{t}_0$ the prescribed traction on Γ_{nu}, θ_0 the given temperature on Γ_{dt} and α, g, and θ_1 the thermal conduction coefficient, the prescribed heat flux and the ambient temperature on Γ_{nt}, respectively. The boundary conditions to be considered are

$$\mathbf{u} = \mathbf{u}_0 \qquad \text{on } \Gamma_{du} \tag{6}$$

$$\mathbf{n} \cdot \boldsymbol{\sigma} = \mathbf{t}_0 \qquad \text{on } \Gamma_{nu} \tag{7}$$

$$\theta = \theta_0 \qquad \text{on } \Gamma_{dt} \tag{8}$$

$$-k\mathbf{n} \cdot \nabla\theta = g + \alpha(\theta - \theta_1) \qquad \text{on } \Gamma_{nt} \tag{9}$$

In order to write the weak form of the problem described by (1), (2), (4) and (6)–(9), let V_u, V_p and V_t be the appropriate spaces of trial functions for the velocity, the pressure and the temperature, respectively, and W_u, W_p and W_t the spaces of weighting functions. The weak form of the problem we consider is: find a velocity field $\mathbf{u} \in V_u$, a pressure $p \in V_p$ and a temperature $\theta \in V_t$ such that

$$2\int_\Omega \mu\boldsymbol{\varepsilon}(\mathbf{u}) : \boldsymbol{\varepsilon}(\mathbf{v})\, d\Omega - \int_\Omega p\nabla \cdot \mathbf{v}\, d\Omega = \rho\int_\Omega \mathbf{f} \cdot \mathbf{v}\, d\Omega + \int_{\Gamma_{nu}} \mathbf{t}_0 \cdot \mathbf{v}\, d\Gamma \tag{10}$$

$$\int_\Omega q\nabla \cdot \mathbf{u}\, d\Omega = 0 \tag{11}$$

$$k\int_\Omega \nabla\theta \cdot \nabla\eta\, d\Omega + \rho c\int_\Omega (\mathbf{u} \cdot \nabla\theta)\eta\, d\Omega = 2\int_\Omega \mu\boldsymbol{\varepsilon}(\mathbf{u}) : \boldsymbol{\varepsilon}(\mathbf{u})\eta\, d\Omega + \int_{\Gamma_{nt}} [g + \alpha(\theta - \theta_1)]\eta\, d\Gamma \tag{12}$$

for all $\mathbf{v} \in W_u$, $q \in W_p$ and $\eta \in W_t$.

The constitutive law of the fluid will enter the problem described by (10)–(12) through an equation relating the viscosity with the temperature and the invariants of $\boldsymbol{\varepsilon}(\mathbf{u})$. Let us write, symbolically,

$$\mu = \mu(\theta, \boldsymbol{\varepsilon}(\mathbf{u})) \tag{13}$$

At the end of the paper we will present some numerical experiments for a particular case of (13), namely, for the power law with an exponential-type thermal dependence.

Finite element discretization

Let $\{\Omega_e\}$ be a finite element discretization of the domain Ω, with subscript e ranging from 1 to the number of elements N_{el}. For each element, denote by N_{nu}, N_{np} and N_{nt} the number of nodes with velocity, pressure and temperature degrees of freedom, respectively. The discrete version of the problem described by (10)–(12) leads to the following algebraic system:

$$\mathbf{K}(\mu)\mathbf{U} - \mathbf{G}\mathbf{P} = \mathbf{F}_u \tag{14}$$

$$\mathbf{G}^T\mathbf{U} = \mathbf{F}_p \tag{15}$$

$$\mathbf{H}(\mathbf{u})\boldsymbol{\Theta} = \mathbf{F}_t(\mu, \mathbf{u}) \tag{16}$$

We have explicitly indicated the dependence of the matrices and vectors in the above equations on the viscosity and the velocity. Capital letters $\mathbf{U}$, $\mathbf{P}$ and $\boldsymbol{\Theta}$ denote the vector of nodal unknowns of the corresponding lower-case variables. The expression of the matrices $\mathbf{K}$, $\mathbf{G}$ and $\mathbf{H}$ and the vectors $\mathbf{F}_u$ and $\mathbf{F}_t$ can be consulted in any standard finite element text book (see e.g. References 6, 7, 1). The vector $\mathbf{F}_p$ comes from the imposition of the Dirichlet boundary condition (6) for the velocity field.

Consider first the case in which the viscosity μ does not depend on the temperature θ. Under this assumption, equations (14) and (15) are uncoupled with equation (16), that can be solved once $\mathbf{U}$ is known. If the viscosity μ is constant (Newtonian fluid), it is well known that the discrete velocity space $V_{u,h}$ and pressure space $V_{p,h}$ must satisfy the discrete Babuška–Brezzi (BB) stability condition.[8] When the viscosity depends on the invariants of the strain-rate tensor $\boldsymbol{\varepsilon}(\mathbf{u})$, the question is whether this condition will be sufficient for assessing stability and convergence of the finite element scheme. In Reference 9, it was proved that, for the case in which the viscosity obeys the power law or the Carreau model, stable and convergent velocity–pressure pairs for the Stokes problem with μ constant are also stable for the non-linear case. Concerning the convergence of the method, let h be the diameter of $\{\Omega_e\}$ and suppose that the rate of convergence for the velocity is of order h^m for Newtonian flows. Assume now that μ satisfies the power law with rate of sensitivity r, with $0 < r < 1$. Then the rate of convergence for the velocity will be of order h^{mr}. For the Carreau model, the same rate of convergence as for the constant viscosity case can be obtained. See Reference 9 for details.

Based on the results stated above, finite element interpolations for the velocity and the pressure that are known to satisfy the discrete Babuška–Brezzi condition have been employed. See References 7 and 1 for a fairly complete description of available interpolations and Reference 10 for the analysis of the elements. As will be shown later, we will be interested in discontinuous pressure interpolations. For the numerical examples presented later, we have used the Q_2/P_1 element, constructed using a continuous biquadratic or triquadratic (in 2-D or 3-D) velocity interpolation and discontinuous piecewise linear pressures. We have also obtained excellent answers with the $P2^+/P1$ element (continuous quadratic velocities enriched with bubble functions, discontinuous piecewise linear pressures). Both the Q2/P1 and the $P2^+/P1$ elements are known to have optimal rates of convergence.[10]

Concerning the implementation of piecewise linear pressures, two options are possible. If $\mathrm{s} = (s_1, s_2, s_3)$ (in 3-D) are the co-ordinates of the parent domain of the elements, the first choice is to place $N_{sd} + 1 = 4$ nodes within the elements, with co-ordinates s_j, $j = 1, 2, 3, 4$, and construct shape functions $N_i(\mathrm{s})$, $i = 1, 2, 3, 4$, such that $N_i(\mathrm{s}_j) = \delta_{ij}$ (the Kronecker symbol) for $i, j = 1, 2, 3, 4$. Then, if the pressure is interpolated as $p(\mathrm{s}) = \sum_{i=1}^{4} N_i(\mathrm{s}) p_i$, the coefficients p_i, $i = 1, 2, 3, 4$, have the meaning of being the nodal values of the pressure. A simpler option is to interpolate p as $p(\mathrm{s}) = p_0 + s_1 p_1 + s_2 p_2 + s_3 p_3$. Now, p_0 is the value of the pressure for $s_1 = s_2 = s_3 = 0$ and p_1, p_2 and p_3 are its first derivatives. In our computations, we have found no difference in the numerical results using both approaches.

Up to now, we have described the velocity and pressure interpolations. For the temperature, we use the same interpolation as for the components of the velocity. Thus, $N_{nt} = N_{nu}$.

THE ITERATIVE PENALTY METHOD

Description of the method and convergence properties for Newtonian flows

For simplicity, we will assume now the case in which $\mathbf{u}_0 = \mathbf{0}$, μ is constant and Γ_{nu} is the empty set. The matrix form of the problem is now

$$\mathbf{K}(\mu)\mathbf{U} - \mathbf{G}\mathbf{P} = \mathbf{F}_u \tag{17}$$

$$\mathbf{G}^{\mathrm{T}}\mathbf{U} = \mathbf{0} \tag{18}$$

Let $\mathbf{M}$ be any positive-definite (not necessarily symmetric) $n_2 \times n_2$ matrix, n_2 being the total number of pressure unknowns. In particular, $\mathbf{M}$ can be taken as the Gramm matrix whose

components are the inner products of the pressure shape functions N_p:

$$M_{ij} = \int_\Omega N_p^{(i)} N_p^{(j)} \, d\Omega \tag{19}$$

where the superscripts i and j refer to the pressure node. If ε is a small number, the penalty method applied to the problem described by (17) and (18) leads to the following algebraic system:

$$\mathbf{K}(\mu)\mathbf{U}^{\varepsilon(1)} - \mathbf{G}\mathbf{P}^{\varepsilon(1)} = \mathbf{F}_u \tag{20}$$

$$\mathbf{G}^{\mathrm{T}}\mathbf{U}^{\varepsilon(1)} + \varepsilon\mathbf{M}\mathbf{P}^{\varepsilon(1)} = \mathbf{0} \tag{21}$$

Let $\mathbf{U} = \mathbf{U}^{\varepsilon(1)} + \delta\mathbf{U}$ and $\mathbf{P} = \mathbf{P}^{\varepsilon(1)} + \delta\mathbf{P}$ be the solution of the problem described by (17) and (18), where $\mathbf{U}^{\varepsilon(1)}$ and $\mathbf{P}^{\varepsilon(1)}$ is the solution of the problem described by (20) and (21). Subtracting equation (20) from (17) and equation (21) from (18), one finds that

$$\mathbf{K}(\mu)\delta\mathbf{U} - \mathbf{G}\delta\mathbf{P} = \mathbf{0} \tag{22}$$

$$\mathbf{G}^{\mathrm{T}}\delta\mathbf{U} = \varepsilon\mathbf{M}\mathbf{P}^{\varepsilon(1)} \tag{23}$$

This problem can be solved again using the penalty method. Let $\delta\mathbf{U}^{\varepsilon}$ and $\delta\mathbf{P}^{\varepsilon}$ be the penalized solution and define $\mathbf{U}^{\varepsilon(2)} = \mathbf{U}^{\varepsilon(1)} + \delta\mathbf{U}^{\varepsilon}$ and $\mathbf{P}^{\varepsilon(2)} = \mathbf{P}^{\varepsilon(1)} + \delta\mathbf{P}^{\varepsilon}$. We will have that

$$\mathbf{K}(\mu)\mathbf{U}^{\varepsilon(2)} - \mathbf{G}\mathbf{P}^{\varepsilon(2)} = \mathbf{F}_u \tag{24}$$

$$\mathbf{G}^{\mathrm{T}}\mathbf{U}^{\varepsilon(2)} + \varepsilon\mathbf{M}\mathbf{P}^{\varepsilon(2)} = \varepsilon\mathbf{M}\mathbf{P}^{\varepsilon(1)} \tag{25}$$

Applying inductively the same reasoning used to arrive at (24) and (25), the following algorithm is obtained:

Given $\mathbf{P}^{\varepsilon(0)}$, for $i = 1, 2, \ldots$, find $\mathbf{U}^{\varepsilon(i)}$ and $\mathbf{P}^{\varepsilon(i)}$ such that

$$\mathbf{K}(\mu)\mathbf{U}^{\varepsilon(i)} - \mathbf{G}\mathbf{P}^{\varepsilon(i)} = \mathbf{F}_u \tag{26}$$

$$\mathbf{G}^{\mathrm{T}}\mathbf{U}^{\varepsilon(i)} + \varepsilon\mathbf{M}\mathbf{P}^{\varepsilon(i)} = \varepsilon\mathbf{M}\mathbf{P}^{\varepsilon(i-1)} \tag{27}$$

Remarks

(1) The algorithm given by (26) and (27) may be viewed as a variant of the augmented Lagrangian method (see e.g. Reference 11) provided that Uzawa's algorithm is used to update the pressure. This was implicitly done in early works whose basic motivation was also the computational problems encountered when small penalties are used. For example, the method was applied in linear incompressible elasticity in Reference 12 and the discrete algebraic system was considered in Reference 13; see also Reference 14. As will be seen below, we will not require the matrix $\mathbf{K}$ to be symmetric (although it certainly is, for the problem we consider) and, thus, an associated minimization problem is not needed for deriving (26) and (27). For an application of the augmented Lagrangian method to non-Newtonian fluids, see Reference 15.

(2) The residual out-of-balance argument used to arrive at (26) and (27) is completely general and has physical meaning for non-linear cases, either if the non-linearity comes from the momentum equations (Navier–Stokes problem) or from the constitutive law of the material. The step from the problem described by (20) and (21) to that described by (22) and (23) may be applied in non-linear problems as well, although in these cases $\delta\mathbf{U}$ and $\delta\mathbf{P}$ will be the solution of a non-linear problem that in turn has to be linearized. Our leading idea is trying to converge in this process to the true incompressible solution (see the Appendix).

(3) There are possibly many ways for 'rediscovering' the algorithm described by (26) and (27). Another one is to introduce a false transient for the pressure (not for the momentum equation) assuming the fluid to be slightly compressible and then to discretize the temporal derivative using the backward Euler scheme. Except for this discretization, this is nothing but the artificial compressibility method introduced by Chorin.[16] The penalty parameter ε in this case would be the inverse of $c^2\Delta t$, where c is the speed of sound in the fluid and Δt the time step. See Reference 17 for a further discussion.

(4) Looking at the problem described by (20) and (21) we see that the *discrete* incompressibility constraint has been penalized. The pressure interpolation is, thus, independent of the finite element velocity space and stable velocity pressure interpolations can be used. On the other hand, if one starts penalizing the continuous incompressibility constraint and then eliminating the pressure in the momentum equations, the associated pressure space is determined by the velocity space. In general, the resulting velocity–pressure pair will not satisfy the BB stability condition and, in order to obtain stable or semi-stable schemes, reduced or selective integration techniques have to be employed.[18,19] We will not consider these methods in this paper. For a further discussion, see References 19 -23.

Although expressions (26) and (27) will be kept in what follows, their implementation uses the fact that the pressure interpolation is discontinuous. This allows to eliminate the pressure degrees of freedom, thus making the method much more efficient from the computational point of view. For discontinuous pressures, equation (27) holds for each element. If we denote by superscript e the element arrays, we will have

$$\mathbf{G}^{(e)^{\mathrm{T}}}\mathbf{U}^{(e)^{\varepsilon(i)}} + \varepsilon\mathbf{M}^{(e)}\mathbf{P}^{(e)^{\varepsilon(i)}} = \varepsilon\mathbf{M}^{(e)}\mathbf{P}^{(e)^{\varepsilon(i-1)}} \tag{28}$$

and, hence,

$$\mathbf{P}^{(e)^{\varepsilon(i)}} = \mathbf{P}^{(e)^{\varepsilon(i-1)}} - \frac{1}{\varepsilon}\mathbf{M}^{(e)^{-1}}\mathbf{G}^{(e)^{\mathrm{T}}}\mathbf{U}^{(e)^{\varepsilon(i)}} \tag{29}$$

Let $\mathscr{A}$ denote the standard finite element assembly operator. From (26) and (29) we have

$$\left[\mathbf{K}(\mu) + \frac{1}{\varepsilon}\mathscr{A}_{e=1}^{N_{\mathrm{el}}}(\mathbf{G}^{(e)}\mathbf{M}^{(e)^{-1}}\mathbf{G}^{(e)^{\mathrm{T}}})\right]\mathbf{U}^{\varepsilon(i)} = \mathbf{F}_u + \mathbf{G}\mathbf{P}^{\varepsilon(i-1)} \tag{30}$$

Once $\mathbf{U}^{\varepsilon(i)}$ is found by solving equation (30), the pressure nodal values can be computed for each element from expression (29). It should be remarked that the matrix of the system (30) has to be factored only once for Newtonian flows and that the inversion of $\mathbf{M}^{(e)}$ is trivial (it is a $(N_{sd}+1)\times(N_{sd}+1)$ matrix if linear pressures are used).

We now proceed to analyse the convergence of the iterates $\mathbf{U}^{\varepsilon(i)}$, $\mathbf{P}^{\varepsilon(i)}$, solution of the problem described by (26) and (27), to the pure incompressible solution $\mathbf{U}$, $\mathbf{P}$ of the problem described by (17) and (18). Our objective is to use arguments as simple as possible, only involving linear algebra concepts (see Reference 5 for a more abstract approach). Let N_{fn} be the total number of free nodes of the finite element mesh with velocity degrees of freedom. Define $n_1 = N_{sd}\times N_{\mathrm{fn}}$ and $n_2 = N_{\mathrm{el}}\times N_{np}$. We will have that $\mathbf{U}^{\varepsilon(i)}\in\mathbb{R}^{n_1}$ and $\mathbf{P}^{\varepsilon(i)}\in\mathbb{R}^{n_2}$. It is well known that $\mathbf{K}(\mu)$ is a symmetric and positive-definite $n_1\times n_1$ matrix, with components proportional to μ. We will not need its symmetry but only its positive-definiteness and its continuity (it defines a linear mapping in $\mathbb{R}^{n_1}$). Thus, there exist positive constants C_1 and C_2 such that

$$\begin{aligned} C_1\mu\,\|\,\mathbf{V}_1\,\|^2 &\leqslant \mathbf{V}_1^{\mathrm{T}}\mathbf{K}(\mu)\mathbf{V}_1 \\ \mathbf{V}_1^{\mathrm{T}}\mathbf{K}(\mu)\mathbf{V}_2 &\leqslant C_2\mu\,\|\,\mathbf{V}_1\,\|\,\|\,\mathbf{V}_2\,\| \end{aligned} \tag{31}$$

where $\mathbf{V}_1, \mathbf{V}_2 \in \mathbb{R}^{n_1}$ and $\| \cdot \|$ denotes the Euclidian norm in $\mathbb{R}^{n_1}$ or $\mathbb{R}^{n_2}$. For the $n_1 \times n_2$ matrix $\mathbf{G}$, we assume that the following condition holds: for each $\mathbf{Q} \in \mathbb{R}^{n_2}$ there exists a $\mathbf{V} \in \mathbb{R}^{n_1}$, $\mathbf{V} \neq \mathbf{0}$, such that

$$\mathbf{V}^{\mathrm{T}}\mathbf{G}\mathbf{Q} \geqslant C_3 \| \mathbf{V} \| \| \mathbf{Q} \| \tag{32}$$

for a certain positive constant C_3 independent of the mesh diameter h. Condition (32) is the discrete form of the BB stability condition. See Reference 8 for an equivalent formulation.

The final ingredient we need is the fact that $\mathbf{M}$ is also a positive-definite matrix. Thus, there exist positive constants C_4 and C_5 such that

$$\begin{aligned} C_5 \| \mathbf{Q}_1 \|^2 &\leqslant \mathbf{Q}_1^{\mathrm{T}}\mathbf{M}\mathbf{Q}_1 \\ \mathbf{Q}_1^{\mathrm{T}}\mathbf{M}\mathbf{Q}_2 &\leqslant C_4 \| \mathbf{Q}_1 \| \| \mathbf{Q}_2 \| \end{aligned} \tag{33}$$

for any $\mathbf{Q}_1, \mathbf{Q}_2 \in \mathbb{R}^{n_2}$.

Subtracting now equation (17) from (26) and equation (18) from (27), we obtain

$$\mathbf{K}(\mu)(\mathbf{U} - \mathbf{U}^{\varepsilon(i)}) - \mathbf{G}(\mathbf{P} - \mathbf{P}^{\varepsilon(i)}) = \mathbf{0} \tag{34}$$

$$\mathbf{G}^{\mathrm{T}}(\mathbf{U} - \mathbf{U}^{\varepsilon(i)}) + \varepsilon\mathbf{M}(\mathbf{P}^{\varepsilon(i-1)} - \mathbf{P}^{\varepsilon(i)}) = \mathbf{0} \tag{35}$$

On the other hand, from conditions (33) we see that

$$\begin{aligned} 0 &\leqslant (\mathbf{P} - \mathbf{P}^{\varepsilon(i)})^{\mathrm{T}}\mathbf{M}(\mathbf{P} - \mathbf{P}^{\varepsilon(i)}) \\ &= (\mathbf{P} - \mathbf{P}^{\varepsilon(i)})^{\mathrm{T}}\mathbf{M}(\mathbf{P} - \mathbf{P}^{\varepsilon(i-1)}) + (\mathbf{P} - \mathbf{P}^{\varepsilon(i)})^{\mathrm{T}}\mathbf{M}(\mathbf{P}^{\varepsilon(i-1)} - \mathbf{P}^{\varepsilon(i)}) \end{aligned}$$

and, hence,

$$(\mathbf{P} - \mathbf{P}^{\varepsilon(i)})^{\mathrm{T}}\mathbf{M}(\mathbf{P}^{\varepsilon(i)} - \mathbf{P}^{\varepsilon(i-1)}) \leqslant (\mathbf{P} - \mathbf{P}^{\varepsilon(i)})^{\mathrm{T}}\mathbf{M}(\mathbf{P} - \mathbf{P}^{\varepsilon(i-1)}) \tag{36}$$

Multiplying equation (34) by $\mathbf{U} - \mathbf{U}^{\varepsilon(i)}$ and equation (35) by $\mathbf{P} - \mathbf{P}^{\varepsilon(i)}$ and using inequalities (31), (33) and (36), we find that

$$\begin{aligned} C_1\mu \| \mathbf{U} - \mathbf{U}^{\varepsilon(i)} \|^2 &\leqslant (\mathbf{U} - \mathbf{U}^{\varepsilon(i)})^{\mathrm{T}}\mathbf{K}(\mu)(\mathbf{U} - \mathbf{U}^{\varepsilon(i)}) \\ &= (\mathbf{U} - \mathbf{U}^{\varepsilon(i)})^{\mathrm{T}}\mathbf{G}(\mathbf{P} - \mathbf{P}^{\varepsilon(i)}) \\ &= \varepsilon(\mathbf{P} - \mathbf{P}^{\varepsilon(i)})^{\mathrm{T}}\mathbf{M}(\mathbf{P}^{\varepsilon(i)} - \mathbf{P}^{\varepsilon(i-1)}) \\ &\leqslant \varepsilon C_4 \| \mathbf{P} - \mathbf{P}^{\varepsilon(i)} \| \| \mathbf{P} - \mathbf{P}^{\varepsilon(i-1)} \| \end{aligned} \tag{37}$$

Let $\mathbf{V} \in \mathbb{R}^{n_1}$ be such that condition (32) holds for $\mathbf{Q} = \mathbf{P} - \mathbf{P}^{\varepsilon(i)}$. Multiplying equation (34) by this $\mathbf{V}$ and using (31), we obtain

$$\begin{aligned} C_3 \| \mathbf{V} \| \| \mathbf{P} - \mathbf{P}^{\varepsilon(i)} \| &\leqslant \mathbf{V}^{\mathrm{T}}\mathbf{G}(\mathbf{P} - \mathbf{P}^{\varepsilon(i)}) \\ &= \mathbf{V}^{\mathrm{T}}\mathbf{K}(\mu)(\mathbf{U} - \mathbf{U}^{\varepsilon(i)}) \\ &\leqslant C_2\mu \| \mathbf{V} \| \| \mathbf{U} - \mathbf{U}^{\varepsilon(i)} \| \end{aligned} \tag{38}$$

The combination of inequalities (37) and (38) leads to

$$\| \mathbf{U} - \mathbf{U}^{\varepsilon(i)} \| \leqslant (\varepsilon\mu C)\frac{C_3}{\mu C_2} \| \mathbf{P} - \mathbf{P}^{\varepsilon(i-1)} \| \tag{39}$$

$$\| \mathbf{P} - \mathbf{P}^{\varepsilon(i)} \| \leqslant (\varepsilon\mu C) \| \mathbf{P} - \mathbf{P}^{\varepsilon(i-1)} \| \tag{40}$$

where we have defined

$$C = \frac{C_2^2 C_4}{C_1 C_3^2}$$

Applying repeatedly inequalities (39) and (40), we finally get

$$\| \mathbf{U} - \mathbf{U}^{\varepsilon(i)} \| \leqslant (\varepsilon\mu C)^i \frac{C_3}{\mu C_2} \| \mathbf{P} - \mathbf{P}^{\varepsilon(0)} \| \tag{41}$$

$$\| \mathbf{P} - \mathbf{P}^{\varepsilon(i)} \| \leqslant (\varepsilon\mu C)^i \| \mathbf{P} - \mathbf{P}^{\varepsilon(0)} \| \tag{42}$$

From relations (41) and (42) we obtain the following theorem: *there exists a constant C such that if $\bar{\varepsilon} = \varepsilon\mu C < 1$ then the iterates solution of the problem described by (26) and (27) converge to the solution of the problem described by (17) and (18). Moreover convergence is linear with $\bar{\varepsilon}$.*

Let us now discuss some practical consequences of this result. The obvious one is that larger penalty parameters ε can be used for the iterative algorithm described by (26) and (27) than for the standard penalty method. The incompressibility constraint can be approximated up to any given tolerance with a given ε provided that $\bar{\varepsilon} < 1$. The price to be paid is that several iterations of (26) and (27) might be required. However, for large problems this is compensated by the reduction of the number of nodal unknowns with respect to the pure mixed formulation, as explained above. This reduction is especially important in 3-D problems.[24]

It is interesting to observe that convergence is governed by the parameter $\bar{\varepsilon}$, which is proportional to the viscosity μ. This explains why ε must be taken proportional to μ^{-1}, since what provides an idea of how well the incompressibility constraint will be approximated is $\bar{\varepsilon}$, and not ε itself. Of course, this comment can also be applied to the classical penalty method (observe that the first pass in (26) and (27) is nothing but the standard penalty method), and must be kept in mind when one deals with non-constant viscosities.

In practical problems, we have encountered two cases in which the standard penalty method may lead to numerical problems. The first is the one discussed in this work, concerning non-Newtonian flows with variable viscosity. In the numerical examples presented below, it will be seen that the viscosity varies several orders of magnitude in the fluid domain. If a reference viscosity μ_0 is chosen *a priori* for determining a suitable value of ε, it is not known whether this penalty parameter will yield a sufficiently accurate satisfaction of the incompressibility constraint or to ill-conditioning of the final stiffness matrix. Perhaps, another case in which the importance of the variable viscosity is more clear is when the pseudo-concentration method is used to follow free surfaces of creeping flows.[25] The idea of the method is to discretize the whole domain that can be filled by the fluid, assuming that it is occupied either by the fluid itself or by a fictitious material. The physical properties of this fictitious material have to be such that the effect of its motion upon the real fluid can be neglected. In particular, its viscosity must be much smaller than the real one (5 or 6 orders of magnitude is recommended in Reference 25). In our numerical experiments using this method we have found that the standard penalty method leads either to an ill-conditioned stiffness matrix or to a completely unacceptable approximation of the incompressibility constraint, whereas good results can be obtained using the iterative penalization proposed here.

Another issue to be considered is the use of iterative schemes to solve the algebraic system of equations. Due to the high condition number of the final stiffness matrix (see equation (30)), we have found the standard penalty method unfeasible from the practical point of view. In Reference 5, a 3-D cavity flow example is solved using the conjugate gradient method (with a constant viscosity $\mu = 1$). For a problem with 27 783 velocity degrees of freedom, 6303 conjugate gradient

iterations are needed taking $\varepsilon = 10^{-6}$, 2913 for $\varepsilon = 10^{-4}$ and only 418 for $\varepsilon = 10^{-2}$. Of course, more iterations are needed to reach the incompressible solution as ε increases. Nevertheless, the smallest final CPU time is obtained for the largest value of ε. Whether the improvement in the conditioning will be enough or not for using iterative solvers for non-linear problems is something that experience has to provide.

Iterative algorithm for thermally coupled non-Newtonian flows

In order to solve the coupled non-linear system of equations (14)–(16), we use a block iterative algorithm. Let $\mu^{(k,l)}$ denote the viscosity function when the temperature is known at iteration k and the velocity at iteration l. Let TOL be a given tolerance. We check convergence using the criterion $\| \mathbf{U}^{(i)} - \mathbf{U}^{(i-1)} \| < \mathrm{TOL} \| \mathbf{U}^{(i)} \|$. The iterative scheme used is given in Box 1.

Box 1. Algorithm for thermally coupled non-Newtonian flows

- Initialize $\mu^{(0,0)}$, $\mathbf{P}^{(0)}$, $\boldsymbol{\Theta}^{(0)}$
- $i := 0$
- WHILE (*not converged*) DO:
  - $i \leftarrow i + 1$
  - Solve:

$$\mathbf{K}(\mu^{(i-1,i-1)})\mathbf{U}^{(i)} - \mathbf{G}\mathbf{P}^{(i)} = \mathbf{F}_u$$

$$\mathbf{G}^{\mathrm{T}}\mathbf{U}^{(i)} + \varepsilon\mathbf{M}\mathbf{P}^{(i)} = \mathbf{F}_p + \varepsilon\mathbf{M}\mathbf{P}^{(i-1)}$$

  - Update:

$$\mu^{(i-1,i)} = \mu(\theta^{(i-1)}, \mathbf{u}^{(i)})$$

  - Solve:

$$\mathbf{H}(\mathbf{u}^{(i)})\boldsymbol{\Theta}^{(i)} = \mathbf{F}_t(\mu^{(i-1,i)}, \mathbf{u}^{(i)})$$

  - Update:

$$\mu^{(i,i)} = \mu(\theta^{(i)}, \mathbf{u}^{(i)})$$

  - Check convergence:

$$\text{If } \| \mathbf{U}^{(i)} - \mathbf{U}^{(i-1)} \| < \mathrm{TOL} \| \mathbf{U}^{(i)} \| \text{ then } (\textit{converged})$$

END while
END

Remarks

(1) Observe that the thermal problem is solved once the mechanical variables **U** and **P** are known for a certain iteration. There is also the possibility of swapping the order of block iterations. However, for the problems we have considered so far we have found the described option (slightly) more efficient.

(2) The iterative penalization in the above algorithm is coupled with the iterative loop used to deal with the non-linearity of the problem. It will be seen in the numerical experiments presented below that this does not deteriorate the convergence rate of the scheme.

(3) If the viscosity does not depend on the temperature, the algorithm presented is a Picard (or successive substitution) type scheme. This is the most common option in practice.[4,15,3] In fact, convergence problems have been observed when a Newton–Raphson scheme has been

employed in the type of problems we consider (see Reference 6 for further discussion and references therein).

SMOOTHING OF ELEMENT VARIABLES

Least-squares smoothing

In the numerical procedure we have just described, the value of the viscosity has to be stored for each element and for each quadrature point within the element. The pressure nodal values are also located within each element. Both scalar fields will be discontinuous across interelement boundaries. For plotting purposes, it is interesting to obtain a continuous function that approximates a discontinuous one. In our computations, we use a standard least-squares technique,[7,1] which leads to a linear system of the form

$$\mathbf{M}^c\boldsymbol{\Phi} = \mathbf{R} \tag{43}$$

where $\mathbf{M}^c$ is the Gramm matrix arising from the continuous interpolation of the smoothed function ϕ, whose vector of nodal unknowns has been denoted by $\boldsymbol{\Phi}$.

In order to avoid the solution of the linear system (43), it is usual to approximate the matrix $\mathbf{M}^c$ by a diagonal matrix $\mathbf{M}^l$. This matrix can be obtained either by the row-sum lumping technique or by using a nodal quadrature rule to evaluate the integrals appearing in $\mathbf{M}^c$ and $\mathbf{R}$. In this case, the quadrature points are placed on the nodes of the element.

Nodal quadrature rules for linear and quadratic elements

We present in Box 2 some nodal quadrature rules for the most common finite elements used in practice. Some of these rules are well known (rules 1–3, 6–11, 17 in Box 2). Our interest in obtaining the others is not their accuracy but the fact that they allow one to approximate the matrix $\mathbf{M}^c$ in equation (43) by a diagonal matrix.

In Box 2, R_n indicates the rule number and N_{no} the number of nodes of the element. This is followed by a schematic description of the element that has to be precised. For both 2-D and 3-D elements, the bubble function is associated with a node placed at the centre of the element. It is understood that the original shape functions (without the addition of the new node) have to be modified in order to have zero value at the centre. Otherwise, the nodal unknown at this point would not have the meaning of being the value of the interpolated function and the matrix $\mathbf{M}^c$ would not be diagonal. For the element considered in rule number 15, bubble functions are also added in the centre of the faces of the element. Elements corresponding to rules number 1, 2, 5 and 6 are triangular, tetrahedral for rules number 9, 10, 13–15, quadrilateral for rules number 3, 4, 7 and 8 and hexahedral for rules number 11, 12, 16 and 17.

The quadrature rule is defined by the weights of the nodes. All the nodes placed at the corners of the element have the same weight, as well as the nodes placed in the middle of the edges and in the centre of the faces (in 3-D elements). The values given have been normalized in such a way that their sum is 1. In the final entry of Box 2, the accuracy of the quadrature rule is given by the polynomial that can be exactly integrated. The set of polynomials of degree n is denoted by P_n, whereas Q_n denotes the set of tensor-product polynomials of degree n in each Cartesian direction x, y, z.

All the rules except rule number 5 are the best that can be obtained with the given number of quadrature points. In fact, for the 2-D quadratic (simplicial) element, a second-order quadrature rule is obtained if the weights are taken as 0 for the corner nodes and as 1/3 for the mid-side

nodes. However, this rule yields a matrix $\mathbf{M}^{\ell}$, an approximation of $\mathbf{M}^{c}$, with some zero diagonal values (those corresponding to the corner nodes). The weights given for rule number 5 have been obtained by splitting the triangle into four subtriangles and applying rule number 1. It is interesting to remark that if the Richardson extrapolation is applied to rules number 1 and 5, the mentioned second-order rule is recovered.

Box 2. Nodal quadrature rules for linear and quadratic elements

R_n	N_{no}	Description	Weights				Polynomial
Two-dimensional elements							
			Corners	Edges		Centre	
1	3	Linear	1/3				P_1
2	4	Linear + bubble	1/12			3/4	P_2
3	4	Bilinear	1/4				Q_1
4	5	Bilinear + bubble	1/12			2/3	P_2
5	6	Quadratic	1/12	1/4			P_1
6	7	Quadratic + bubble	1/20	2/15		9/20	P_3
7	8	Serendipid	− 1/12	1/3			P_2
8	9	Biquadratic	1/36	1/9		4/9	Q_3
Three-dimensional elements							
			Corners	Edges	Faces	Centre	
9	4	Linear	1/4				P_1
10	5	Linear + bubble	1/20			4/5	P_2
11	8	Trilinear	1/8				Q_1
12	9	Trilinear + bubble	1/24			2/3	P_2
13	10	Quadratic	− 1/120	1/5			P_2
14	11	Quadratic + bubble	1/160	1/15		8/15	P_3
15	15	Quadratic + bubble + face bubbles	17/840	4/105	27/280	32/105	P_3 and terms x^2yz, xy^2z, xyz^2
16	20	Serendipid	− 1/8	1/6			P_2
17	27	Triquadratic	1/216	1/54	2/27	8/27	Q_3

NUMERICAL EXAMPLE

In this section we present some numerical results obtained for the well-known 4:1 plane extrusion problem. All the calculations have been carried out on a CONVEX-C120 computer using double arithmetic precision.

The geometry and the boundary conditions are depicted in Figure 1. The variation of the viscosity and the components of the velocity will be given for sections AA, BB and CC indicated in this figure. The finite element mesh is composed of 525 Q2/P1 elements (biquadratic interpolation for the velocity, piecewise linear pressure), with a total of 2201 nodal points. There are 15 elements in the y-direction from the co-ordinates $y = 3$ to $y = 4$ and only 12 from $y = 0$ to $y = 3$. The concentration of elements in the former zone is needed if one wants to reproduce accurately the shear thinning effect of fluids whose viscosity obeys the power law that we will consider:

$$\mu = K_0(\sqrt{3}\hat{\varepsilon})^{r-1} \exp\left(\frac{\beta}{\theta}\right) \tag{44}$$

In this expression, K_0, r and β are physical constants (K_0 is the material consistency and r the rate

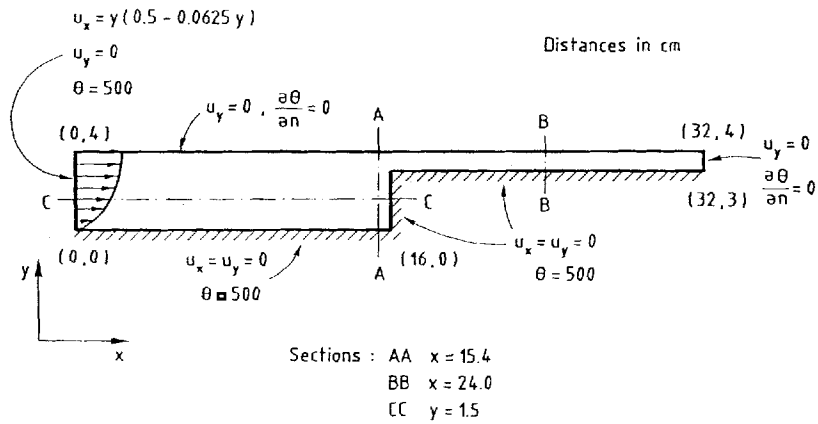

Figure 1. Geometry and boundary conditions for the 4:1 plane extrusion problem

sensitivity), θ is the temperature and $\hat{\varepsilon}$ is defined by

$$\hat{\varepsilon} = \tfrac{2}{3}(\boldsymbol{\varepsilon}(\mathbf{u}):\boldsymbol{\varepsilon}(\mathbf{u}))^{1/2} = \tfrac{2}{3}(2I_2)^{1/2}$$

where I_2 is the second invariant of the strain-rate tensor $\boldsymbol{\varepsilon}(\mathbf{u})$. This expression is a particular case of equation (13).

The values of the physical constants we have used are (all in SI units): $\rho = 1200$ (density), $c = 100$ (specific heat), $k = 2$ (thermal conduction coefficient), $K_0 = 10^6$ (material consistency) and $r = 0{\cdot}2$ (rate sensitivity). For this value of r the effect of the non-constant viscosity is very pronounced. Numerical experiments have also been conducted with larger values of r, in which case convergence is easier to achieve. Since the expression of the viscosity (44) tends to infinity when $\hat{\varepsilon}$ tends to zero, we have introduced a cut-off value $\mu_c = 10^{12}$ for μ. The values of the viscosity for the converged solutions are always below this limit, except in isolated points.

Let us first discuss the performance of the iterative penalization. For values of β between 0 and 2×10^3 the convergence history of the numerical simulation is similar. However, for larger values of β lack of convergence can occur. As proposed in Reference 3, under-relaxation techniques may be required when the dependence of the viscosity on the temperature is very pronounced. The convergence of the algorithm will be discussed in the case in which $\beta = 2 \times 10^3$, that is, when the viscosity depends on the temperature (thermally coupled flow).

Figure 2 shows the evolution of the discrete L^2 norm of the velocity residuals over the norm of the actual velocity (in %), that has been taken as the parameter to decide whether convergence has been achieved or not. Both the curves corresponding to the classical and the iterative penalty methods have been plotted. In the former case, the term $\varepsilon\mathbf{MP}^{(i-1)}$ on the right-hand side of the penalized incompressibility equation of the iterative algorithm is dropped. Here, the penalty parameter that has been used is $\varepsilon = 10^{-13}$. In the first iteration, the viscosity is set to its cut-off value. Thus, the effective initial guess for the second iteration is the Newtonian solution with this viscosity. A real non-Newtonian behaviour will be first encountered in this second iteration and from there onwards iterations are required to reach the prescribed convergence tolerance. However, in Figure 2 we see that one more iteration is needed if the iterative penalization is employed. The explanation we give is that in this method the second pass of the algorithm uses the Newtonian pressures obtained in the first one and, thus, the complete non-Newtonian

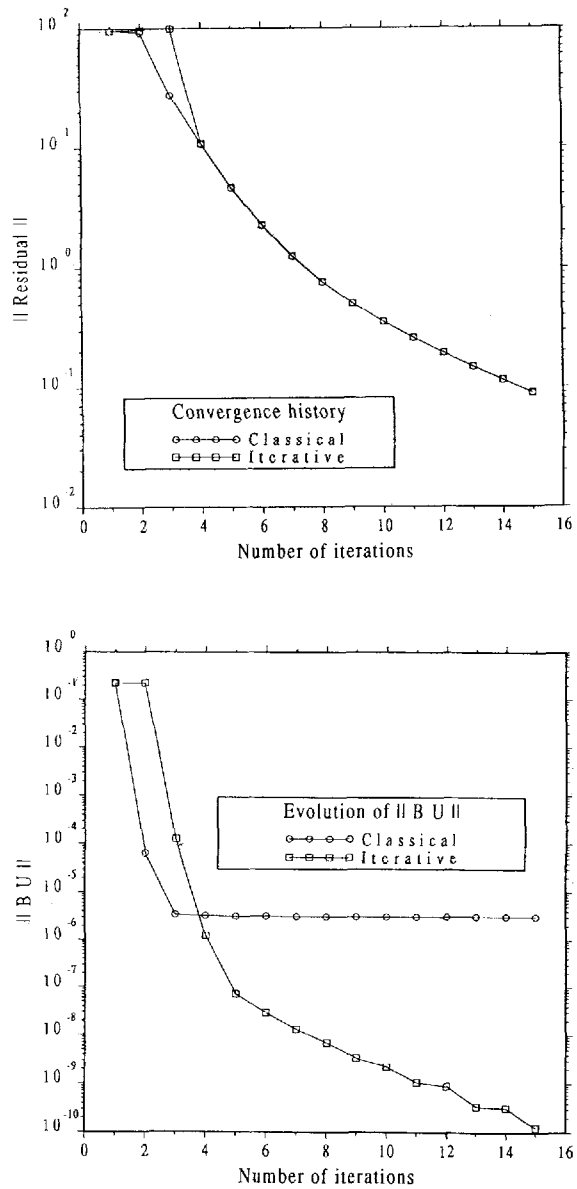

Figure 2. Convergence history and evolution of the norm of the discrete divergence for $\varepsilon = 10^{-13}$

approximation is not obtained until the third iteration. In any case, it is interesting to observe that the final convergence rate and the number of iterations needed to achieve convergence have not been deteriorated because of the iterative penalization.

The important issue is to determine how well the incompressibility constraint has been approximated. If we denote by $\mathbf{B} = \mathbf{G}^{\mathrm{T}}$ the discrete divergence matrix, we should have $\| \mathbf{BU} \| = 0$ in the real incompressible case. The evolution of $\| \mathbf{BU} \|_\infty = \max_i | B_{ij} U_j |$ as the iterative procedure goes on has also been plotted in Figure 2. Observe that this value keeps constant for the

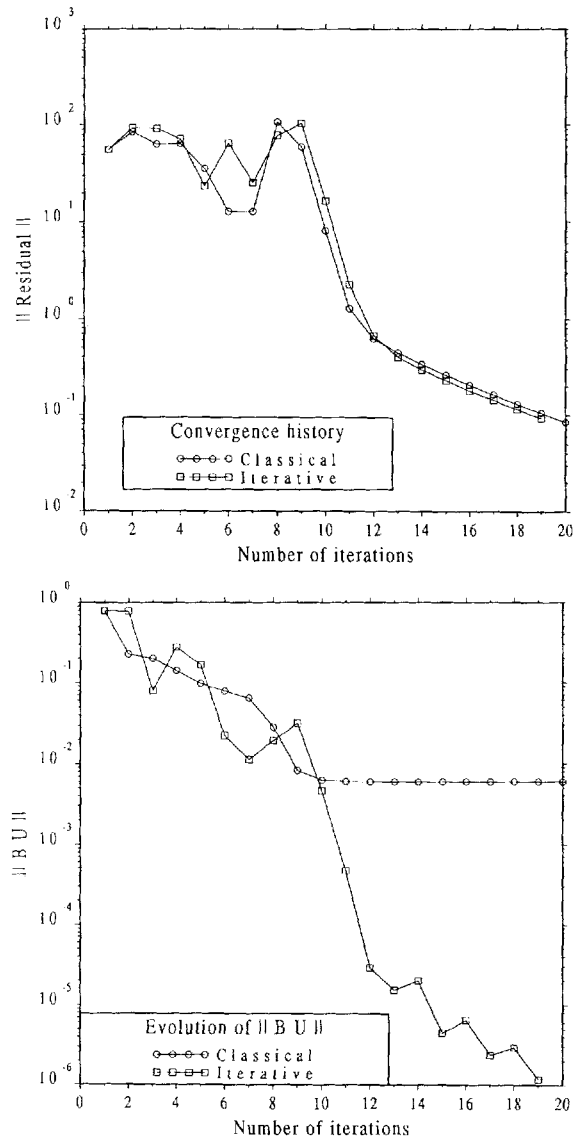

Figure 3. Convergence history and evolution of the norm of the discrete divergence for $\varepsilon = 10^{-10}$

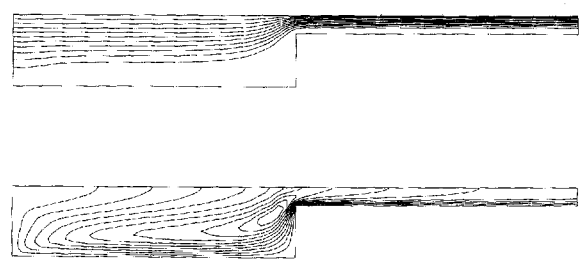

Figure 4. Streamlines and temperature contours ($\beta = 2 \times 10^3$)

classical penalty method and that it decreases uniformly up to a value of order 10^{-10} in 15 iterations if the iterative penalization is used.

The same experiments discussed above have been performed using a penalty parameter $\varepsilon = 10^{-10}$ and the results are presented in Figure 3 (convergence history and evolution of the norm of the discrete divergence). The conclusions are similar to the previous case. Observe now that oscillations are found for the first few iterations and then the iterates converge uniformly.

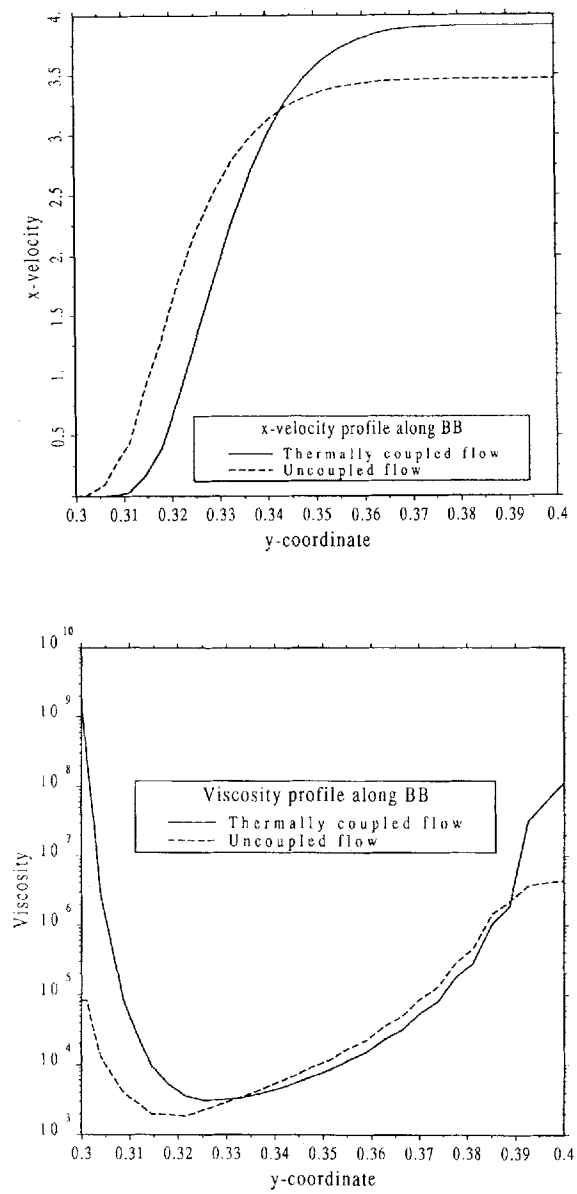

Figure 5. x-velocity and viscosity profiles along section BB for $\beta = 0$ (uncoupled flow) and $\beta = 2 \times 10^3$ (thermally coupled flow)

The reason for this behaviour is the high value of ε, that is of the same order as the inverse of the maximum viscosity, and 100 times higher than μ_c^{-1}, the inverse of the cut-off value. It is observed that the incompressibility constraint is poorly approximated using the classical penalty method.

The physical results for this problem are presented in Figures 4–6 (co-ordinates are given in decimetres). Figure 4 shows the streamlines and the temperature contours for $\beta = 2 \times 10^3$. From equations (4) and (5) it is clear that the temperature will rise where the internal mechanical work is higher, that is, in the zones with high strain rate. This happens near the corner $(x, y) = (16, 3)$. Figure 5 shows the variation of the x-velocity component and the viscosity along section BB. The

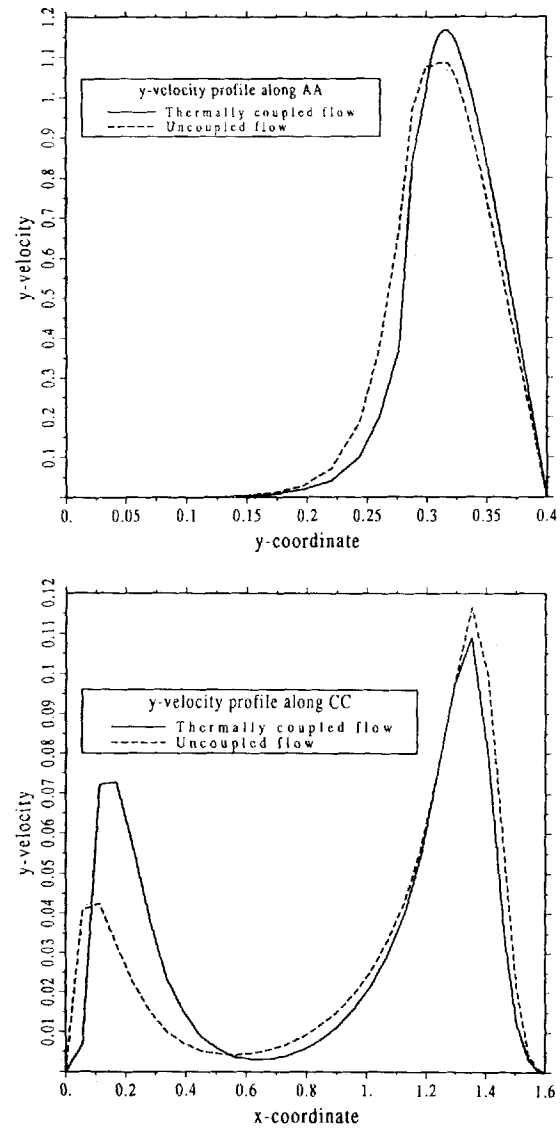

Figure 6. y-velocity profiles along sections AA and CC for $\beta = 0$ (uncoupled flow) and $\beta = 2 \times 10^3$ (thermally coupled flow).

shear thinning effect is very pronounced. The variation of the y-velocity component along sections AA and CC is shown in Figure 6.

CONCLUSIONS

In this paper, a numerical procedure for the finite element solution of viscous non-Newtonian creeping flows using the penalty method has been described. We have discussed the problems associated with the classical penalty method and an iterative version has been introduced. We believe that this approach may help to alleviate some of the drawbacks of the classical method without any significant computational cost.

Although approaches similar to the iterative penalty method have been used before, our motivation has been based on a residual argument, valid for non-linear problems and for cases in which the stiffness matrix is not symmetric. We have also presented a simple convergence analysis for the linear problem, which explains why the penalty parameter ε must be taken proportional to the inverse of the viscosity. Numerical experiments have demonstrated that the *ad hoc* extension to non-linear fluids, whose analysis escapes us, is effective.

Some other related issues have also been treated, such as the block iterative scheme used to couple the thermal and the mechanical problems and the smoothing technique utilized in order to obtain continuous viscosity and pressure fields. Nodal quadrature rules for the most common finite elements used in practice have also been given to apply effectively this method.

APPENDIX

In order to get more insight on the iterative penalty method when dealing with non-linear problems, we consider here the system of equations

$$\begin{aligned} A(x)x + By &= f \\ B^{\mathrm{T}}x &= 0 \end{aligned} \tag{45}$$

where x and y are vectors of nodal unknowns (the bold notation has been abandoned) and A and B are matrices, the former depending on the unknown x.

For simplicity, we assume that system (45) is solved by using the simplest fixed-point or Picard scheme. Let $(x^{(i-1)}, y^{(i-1)})$ be a given guess for (x, y). The differences between this guess and the exact solution, $\delta x := x - x^{(i-1)}$, $\delta y := y - y^{(i-1)}$, will be the solution of

$$\begin{aligned} A(x^{(i-1)} + \delta x)\delta x + B\delta y &= f - A(x^{(i-1)} + \delta x)x^{(i-1)} - By^{(i-1)} \\ B^{\mathrm{T}}\delta x &= -B^{\mathrm{T}}x^{(i-1)} \end{aligned} \tag{46}$$

The main idea behind the Picard scheme is to approximate $A(x^{(i-1)} + \delta x) \approx A(x^{(i-1)})$. Thus, we are led to

$$\begin{aligned} A(x^{(i-1)})\delta\bar{x} + B\delta\bar{y} &= f - A(x^{(i-1)})x^{(i-1)} - By^{(i-1)} \\ B^{\mathrm{T}}\delta\bar{x} &= -B^{\mathrm{T}}x^{(i-1)} \end{aligned}$$

$\delta\bar{x}$ and $\delta\bar{y}$ being approximations to δx and δy, respectively. The second step now is to solve for $\delta\bar{x}$ and $\delta\bar{y}$ using the penalty method. With the notation used in the main text, we will have to find $\delta\bar{x}^{\varepsilon}$ and $\delta\bar{y}^{\varepsilon}$ such that

$$\begin{aligned} A(x^{(i-1)})\delta\bar{x}^{\varepsilon} + B\delta\bar{y}^{\varepsilon} &= f - A(x^{(i-1)})x^{(i-1)} - By^{(i-1)} \\ B^{\mathrm{T}}\delta\bar{x}^{\varepsilon} + \varepsilon M\delta\bar{y}^{\varepsilon} &= -B^{\mathrm{T}}x^{(i-1)} \end{aligned} \tag{47}$$

If we define $x^{(i)} := x^{(i-1)} + \delta\bar{x}^{\varepsilon}$, $y^{(i)} := y^{(i-1)} + \delta\bar{y}^{\varepsilon}$, system (47) may be rewritten as

$$A(x^{(i-1)})x^{(i)} + By^{(i)} = f$$

$$B^{\mathrm{T}}x^{(i)} + \varepsilon My^{(i)} = \varepsilon My^{(i-1)}$$

that is, the Picard algorithm has been coupled with the iterative penalization. So, we see that the two steps used to arrive from the original system (46) to (47) are

(i) approximate $A(x^{(i-1)} + \delta x) \approx A(x^{(i-1)})$ and
(ii) solve *for the increments* using the penalty method.

It is clear that whenever the algorithm is convergent, it will converge towards the solution of (45). On the other hand, if the classical penalty method is employed, system (45) has to be modified *a priori*. In this approach, step (ii) in the above development is clearly missing.

REFERENCES

1. O. C. Zienkiewicz and R. L. Taylor, *The Finite Element Method*, (4th edn.,) Vol. 1, McGraw-Hill, New York, 1989.
2. T. J. R. Hughes, W. K. Liu and A. Brooks, 'Finite element analysis of incompressible viscous flows by the penalty function formulation', *J. Comput. Phys.*, **30,** 1–60 (1979).
3. O. C. Zienkiewicz, E. Oñate and J. C. Heinrich, 'A general formulation for coupled thermal flow of metals using finite elements', *Int. j. numer. methods eng.*, **17,** 1497–1514 (1981).
4. G. F. Carey, K. C. Wang and W. C. Joubert, 'Performance of iterative methods for Newtonian and generalized Newtonian flows', *Int. j. numer. methods fluids*, **9,** 127–150 (1989).
5. R. Codina, 'A finite element model for incompressible flow problems', *Doctoral Thesis*, Universitat Politècnica de Catalunya, 1992.
6. C. Cuvelier, A. Segal and A. van Steenhoven, *Finite Element Methods and Navier–Stokes Equations*, Reidel Dordrecht, 1986.
7. T. J. R. Hughes, *The Finite Element Method. Linear Static and Dynamic Analysis*, Prentice-Hall, Englewood Cliffs, N.J., 1987.
8. F. Brezzi and K. J. Bathe, 'A discourse on the stability conditions for mixed finite element formulations', *Comput. Methods Appl. Mech. Eng.*, **82,** 27–57 (1990).
9. J. Baranger and K. Najib, 'Analyse numérique des écoulements quasi-Newtoniens dont la viscosité obéit à la loi puissance ou à la loi de carreau', *Numer. Math.*, **58,** 35–49 (1990).
10. V. Girault and P. A. Raviart, *Finite Element Methods for Navier–Stokes Equations*, Springer, Berlin, 1986.
11. R. Glowinski, *Numerical Methods for Nonlinear Variational Problems*, Springer, Berlin, 1984.
12. E. M. Salonen, 'An iterative penalty function method in structural analysis', *Int. j. numer. methods. eng.*, **10,** 413–421 (1976).
13. C. A. Felippa, 'Iterative procedures for improving penalty function solutions of algebraic systems', *Int. j. numer. methods eng.*, **12,** 821–836 (1978).
14. O. C. Zienkiewicz, J. P. Vilotte, S. Toyoshima and S. Nakazawa, 'Iterative method for constraint and mixed approximation; an inexpensive improvement of FEM performance,' *Comput. Methods Appl. Mech. Eng.*, **51,** 3–29 (1985).
15. P. Hurez, P. A. Tanguy and F. H. Bertrand, 'A finite element analysis of die swell with pseudoplastic and viscoplastic fluids', *Comput. Methods Appl. Mech. Eng.*, **86,** 87–103 (1991).
16. A. J. Chorin, 'A numerical method for solving incompressible viscous flow problems', *J. Comput. Phys.*, **2,** 12–26 (1967).
17. J. C. Heinrich and B. R. Dyne, 'On the penalty method for incompressible fluids', in E. Oñate, J. Periaux and A. Samuelson (eds.), *Finite Elements in the 90's*, Springer, CIMNE, Barcelona, 1991.
18. J. T. Oden, 'RIP-methods for Stokesian flows', in R. H. Gallagher, D. H. Norrie, J. T. Oden and O. C. Zienkiewicz (eds.), *Finite Elements in Fluids*, Vol. 4, Wiley, New York, 1982.
19. J. T. Oden, N. Kikuchi and Y. J. Song, 'Penalty-finite element methods for the analysis of Stokesian flows', *Comput. Methods Appl. Mech. Eng.*, **31,** 297–329 (1982).
20. M. S. Engelman, R. L. Sani, P. M. Gresho and M. Bercovier, 'Consistent vs. reduced integration penalty methods for incompressible media using several old and new elements', *Int. j. numer. methods fluids*, **2,** 25–42 (1983).
21. M. Fortin, 'Old and new finite elements for incompressible flows', *Int. j. numer. methods fluids*, **3,** 347–364 (1981).
22. C. Johnson and J. Pitkaranta, 'Analysis of some mixed finite element methods related to reduced integration', *Math. Comput.*, **38,** 375–400 (1982).
23. D. S. Malkus and T. J. R. Hughes, 'Mixed finite element methods-reduced and selective integration techniques: a unification of concepts', *Comput. Methods Appl. Mech. Eng.*, **15,** 63–81 (1978).
24. M. P. Robichaud, P. Tanguy and M. Fortin, 'An iterative implementation of the Uzawa algorithm for 3-D fluid flow problems', *Int. j. numer. methods fluids*, **10,** 429–442 (1990).
25. E. Thompson, 'Use of pseudo-concentrations to follow creeping viscous flows during transient analysis', *Int. j. numer. methods fluids*, **6,** 749–761 (1988).